NASA TECHNICAL MEMORANDUM

NASA TM X-52981

NASA TM X-52981

THE EFFECT OF HYPERVELOCITY PROJECTILE MATERIAL ON THE ULTIMATE REFLECTANCE OF BOMBARDED POLISHED METALS

by M. J. Mirtich and H. Mark
Lewis Research Center
Cleveland, Ohio

TECHNICAL PAPER proposed for presentation at
Spring Meeting of the Optical Society of America
Tucson, Arizona, April 5-8, 1971

E-6199

THE EFFECT OF HYPERVELOCITY PROJECTILE MATERIAL ON THE ULTIMATE REFLECTANCE OF BOMBARDED POLISHED METALS

by M. J. Mirtich and H. Mark

Lewis Research Center

E-6199

ABSTRACT

A 76 mm shock tube was used to expose quantitatively various polished metals to hypervelocity impact by micrometer-size projectiles of different compositions, including meteorite material. Spectral reflectance measurements (0.33 to 15.5 μM) were made on the exposed samples using an integrating sphere and a heated black body cavity. The samples were exposed to the projectiles until additional exposure produced no further change in reflectance. In this manner, the effect of the projectile and the projectile-target combination on ultimate reflectance was found. The differences in ultimate reflectance for different materials indicated the importance of proper selection of projectile material for simulating optical degradation of surfaces by micrometeors. The results of this study indicated that stoney type projectiles rather than metallic should be used in ground studies to simulate the effects of micrometeoroids on the optical properties of polished metals.

INTRODUCTION

One of the most difficult space environments to simulate in ground studies has been the near earth micrometeoroid environment, due in part to the lack of a complete knowledge of the micrometeoroid environment itself. Although many micrometeoroid sensors have been sent up into space to measure the flux[1] and a few to measure the speeds of micrometeoroids[2] none have been able to determine the material composition of micrometeoroids. Without information on the composition of micrometeoroids it becomes very difficult to draw conclusions from microparticle impaction studies unless additional investigations are made to determine the importance of the composition of micrometeoroids.

Since spacecraft surface optical properties are often an important mission consideration a program was undertaken at the Lewis Research Center to determine how important the composition of micrometeoroids in ground simulation studies might be in determining the degradation of the optical properties of spacecraft materials. This was accomplished by accelerating various micrometer size particles (that size which is most frequently encountered in space and causes erosion of optical properties of materials) to 2.65 km/sec and impacting these projectiles against various polished metal targets. The reflectance was measured both before and after exposure to the projectiles. The results of these studies, along with the methods used to make these studies are presented herein.

OPTICAL DEGRADATION OF IMPACTED SURFACES

If a polished metal surface is hit by a microparticle at hypervelocity, a crater which is roughly hemispherical is left in the surface. The volume of the crater depends on the target material and has been shown in Ref. 3 (for the speeds considered in this study) to vary directly with the kinetic energy of the projectile. The area of surface damage depends on the crater volume. In Ref. 4 it was found that the resulting total reflectance of the surface could be described in terms of a replacement of the original average reflectance $\overline{\rho}_i$ over the area of damage only by a new reflectance value $\overline{\rho}_\infty$ (ultimate reflectance). From these considerations the following expression was derived to determine the change in reflectance of a polished metal after exposure to hypervelocity projectiles:

$$\overline{\rho}_f(\varepsilon) = \overline{\rho}_i\left[1 - \left(1 - \frac{\overline{\rho}_\infty}{\overline{\rho}_i}\right)\left(1 - e^{-K\varepsilon}\right)\right] \tag{1}$$

where $\overline{\rho}_f(\varepsilon)$ is the average reflectance of the surface after exposure to the total kinetic energy of particles $\varepsilon = \sum_i \frac{1}{2} M_i V_i^2$ hitting the surface, As ε gets very large Eq. (1) reduces to

$$\overline{\rho}_f(\varepsilon) = \overline{\rho}_\infty \tag{2}$$

Thus, the value of $\overline{\rho}_\infty$ can be found by exposing a polished metal until a value of reflectance is reached $(\overline{\rho}_\infty)$ such that further increase in exposure energy produces no further decrease in the measured reflectance. The value of $\overline{\rho}_\infty$ not only is necessary for correctly predicting the reflectance, $\overline{\rho}_f(\varepsilon)$, of a metal for a given exposure energy using Eq. (1), but can also be used to determine the effect of the projectile and target material on reflectance.

EXPERIMENTAL PROCEDURE

The experimental procedure followed was first to measure the reflectance of the samples in an integrating sphere and a heated black body cavity to obtain baseline data. The samples were then placed in the shock tube, exposed quantitatively to a known energy of particles, removed from the shock tube and the reflectance remeasured.

Targets and Projectiles

The metal targets (23.9 mm diameter disks, 1.59 mm thick) used in these studies were soft and hard aluminum, stainless steel, magnesium, titanium, and hard and soft copper. The projectiles used were silicon

carbide (SiC), zirconium dioxide (ZrO_2), silicon dioxide (SiO_2), aluminum oxide (Al_2O_3), iron (Fe) nickel (Ni) and a meteorite, found in Potter, Nebraska in 1941.

These projectile materials were readily available, easy to work with (resistant to static charge build up and moisture, thus preventing agglomeration problems), and thought to be representative of the possible composition of real micrometeoroids.[2] The effects of target exposure to both stoney type projectiles and metal projectiles was considered important and hence investigated. The target materials were considered those commonly used in space application.

Particle Accelerator

A 76 millimeter shock tube was used to accelerate clouds of particles to 2.65 km/sec (Ref. 4). The mass and velocity of the particles were measured so that the total kinetic energy of the particles $\left(\varepsilon = \sum_i \frac{1}{2} M_i V_i^2\right)$ could be used to characterize the exposure of the samples to bombardment. The total kinetic energy used herein is the sum of the energy of successive exposures in the shock tube. For the metal targets used in these studies, the projectiles had sufficient velocity to produce hypervelocity impact effects (Refs. 4 to 6). For such impacts, the craters formed in the metal targets are larger than the impacting projectile if projectile density is of the order of target density. For example at 2.65 km/sec the crater diameter in the metal is about 1.5 times as large as the impacting projectile (Ref. 5). Of course depending on the cratering energy density of the target (hardness) (a value contained in the constant K in Eq. (1)) the craters can be larger or smaller than 1.5 times the projectiles at a projectile velocity of 2.65 km/sec. This can be seen in figure 1(a) and (b). In this figure is presented a photomicrograph (X315) of two surfaces, (a) soft aluminum and (b) hard aluminum both exposed to (2-14) micrometer SiC particles. The craters left in the soft aluminum sample appear larger in size than in the hard aluminum sample (i.e., the cratering energy density of soft aluminum is lower than that of hard aluminum.)

Monochromator-Integrating Sphere

The spectral reflectance of the samples was measured in the spectrum between 0.33 and 2.16 micrometers (μM) using the same monochrometor-integrating sphere system used in Ref. 7. The sample was mounted in the center of the sphere with the incident beam 10 degrees off normal incidence. As a result the first reflection is trapped totally in the sphere, and the total energy reflected from the sample can be measured. The ratio of the signal measured with the beam incident on the sample to that measured with the beam incident on the wall of the sphere gives the fraction of energy reflected. Before this approach was accepted, the effects of angle of incidence and of the polarization of the incident beam on the sample properties were investigated. The angle of incidence was varied

from 8 to 20 degrees off normal incidence and was found to have very little effect on the measured value of reflectance. To assure that there were no effects due to polarization, measurements were made with the sample in the conventional orientation and with the sample rotated 90° with respect to the incident beam. No discernible effects were measured. With the sample normal to the incident beam from the monochromator the diffuse reflectance of the surface can be determined.

Infrared Spectrometer

Spectral infrared reflectance measurements of the samples were made from 1.5 to 15.5 micrometers with an infrared spectrometer coupled with a heated-cavity black body (hohlraum system). In such a system, the spectrometer compares the radiation at a given wavelength from a 600° C black body cavity with the radiation reflected from the water cooled sample within the cavity.

DEGRADATION OF REFLECTANCE WITH EXPOSURE

Figure 2 shows the effects of the exposure to $\overline{6}$ micrometer SiC particles (Note: the average size of the SiC particles was 6 micrometer, for a size distribution of 2 to 14 micrometers) on the spectral reflectance between 0.33 to 2.16 μM of a polished hard aluminum (7075) disk. The sample was exposed to successive bombardment by the $\overline{6}$ μM SiC particles until no further charge in reflectance (i.e., ultimate reflectance) of the sample took place with increased exposure. The spectral reflectance of the sample decreases uniformally at all wavelengths with successive exposures and for the first two exposures, $\varepsilon_1 \doteq 0.908$ joules and $\varepsilon_2 = 1.24$ joules, the reduction in reflectance appears to retain the spectral characteristics of the unexposed hard aluminum. However, at the exposure level where the ultimate reflectance is reached (in this case $\varepsilon = 32$ joules), the characteristic absorption band of aluminum disappears and a spectral reflectance that looks neither like that of SiC powder[8] or polished aluminum appears. Although not presented here, the same type of spectral changes between 0.33 to 2.16 μM occur when titanium, stainless steel and hard aluminum 2024 are exposed to $\overline{6}$ μM SiC particles.

Presented in figure 3 is the reflectance (specular plus diffuse) as a function of wavelength (1.5 to 15.5 μM) for a polished hard aluminum (2024) disk both before and after exposure to $\overline{6}$ μM SiC particles. Here the reflectance of the sample was measured in the infrared using the hohlraum reflectometer. The exposure energy varied from an initial value of $\varepsilon_1 = 1.21$ joules to a final exposure of 27 joules. Unlike the uniform spectral reduction of reflectance of the sample in figure 2, measured between 0.33 and 2.16 micrometers, here the reduction in reflectance is not the same at all wavelengths. The reduction is more in the near infrared than in the far infrared, and the reflectance does not retain the

spectral characteristics of the unexposed specimen. Although not presented herein, diffuse reflectance measurements were made on the sample materials shown in figures 2 and 3. Before exposure to the particles the total reflectance is almost totally specular, but as the exposure energy increases the total reflectance becomes more diffuse and less specular, until at the ultimate reflectance it is totally diffuse.

In order to present the spectral values of the ultimate reflectance in a more meaningful fashion, so that comparisons can be made, a total (wavelength independant) reflectance value was determined by integrating the spectral reflectance and weighting it for radiation from a black body at 420 K. This normalization temperature was picked because 420 K is the equilibrium temperature of a polished metal surface left a 1. A.U. in interplanetary space (but not near the earth). If the solar reflectance were desired, the spectral reflectance of the samples could be integrated and weighted for a 6000 K black body. When this was done on some of the exposed samples it was found that for the energy distribution function of the 6000 K black body and spectral values of the present samples, the integrated values do not change relative to each other, and hence the results presented herein will not change significantly. Thus, the total reflectance is defined here as

$$\bar{\rho}_f = \frac{\int_{\lambda_1}^{\lambda_2} \rho(\lambda)\phi_{B.B.}(\lambda)d\lambda}{\int_{\lambda_1}^{\lambda_2} \phi_{B.B.}(\lambda)d\lambda} \tag{3}$$

for $\lambda_1 = 1.5$ micrometers and $\lambda_2 = 15.5$ micrometers. (For normalization to a 420 K black body, values of λ below 1.5 micrometers were neglected.) This average reflectance characterizes the optical condition of the surface and is used to determine the effect of exposure on the ultimate reflectance.

In figure 4(a) the ultimate reflectance of various disk target materials is presented for various projectile materials. The projectiles used and their average size were: 60 μM SiO_2 (glass microballons), 6 μM SiC, 15 μM ZrO_2, 7 μM Fe, 2.5 μM Ni, and a real meterorite, the Potter, Nebraska meteorite, that was ground to an average size of 1.87 micrometers. Only the average size for each particle is presented, although all the particles used had a size distribution. For a given projectile, the values of $\bar{\rho}_\infty$ are seen to vary with target material. For SiC, Fe, Ni, and Potter, Nebraska projectiles the values of $\bar{\rho}_\infty$ vary less from target to target than they do for targets exposed to 60 μM SiO_2 (hollow glass microballons), where these values range from as little as 0.27 for a magnesium target to as high as 0.58 for a titanium target; a change greater than one hundred percent. The variation in $\bar{\rho}_\infty$ for the targets exposed to 15 μM ZrO_2 particles, is similar to those of the SiC, Fe, Ni, and Potter, Nebraska projectiles except for the low value of the

titanium sample. Hence, in this study the value of ultimate reflectance is not that of the projectile reflectance, since for a given projectile, a variation of reflectance with target does exist.

Obtaining the values of ultimate reflectance is very time consuming, requiring repeated exposures in the shock tube and measurements of the spectral reflectance after the exposure. Hence, not all the targets were exposed to each of the different types of projectiles used in the experiment.

To get a better picture of the effect of the projectile on the target, a grouping by target of the ultimate reflectance after exposure to various projectiles is plotted in figure 4(b) for hard aluminum, soft aluminum, stainless steel and hard copper. This figure shows that the value of $\overline{\rho}_\infty$ for a given target material is not altogether independant of projectile material. This figure permits one to compare more easily the values of $\overline{\rho}_\infty$ for the various projectiles with that of the Potter, Nebraska meteorite. The Potter, Nebraska meteorite is made up of stoney material and hence it is not surprising that the values of $\overline{\rho}_\infty$ obtained in the aluminum targets for SiC, ZrO_2, Al_2O_3 and SiO_2 are very close to those for the Potter, Nebraska meteorite. For the stainless steel targets the values of $\overline{\rho}_\infty$ (0.34) for SiC and ZrO_2 are close, but there was an exception, for the 60 μM SiO_2 particles (glass microballons). These produced a relatively high value of $\overline{\rho}_\infty$ (0.54) that was similar to that obtained with Fe and Ni particles. This test was repeated several times, starting with other unexposed stainless steel targets, with the resulting values of $\overline{\rho}_\infty$ remaining unchanged. Changing the size of the SiC projectile from 6 μM to 1.5 μM had no effect on the ultimate reflectance of hard aluminum. The different types of projectiles used for the exposures varied in size from 1/2 μM for Al_2O_3 to 60 μM for the hollow SiO_2; there seemed to be no effect of size on $\overline{\rho}_\infty$ for a given type of projectile (stoney or metal). An important result of the exposures, is that the metallic projectiles, 2.5 μM Fe and 7 μM Ni, give higher values of $\overline{\rho}_\infty$ than do the stoney type of projectiles. Thus, if the Potter, Nebraska meteorite (stoney) is considered representative of the composition of micrometeoroids, metallic projectiles should not be used to find the effects of micrometeoroids on the reflectance of metals.

Verniani (Ref. 9) in a comprehensive analysis gave an average density of 0.5 grams/cm^3 for meteoritic particles of photographic magnitude of +8, corresponding to particle mass values in the range of 10^{-3} to 10^{-4} gram. It is generally believed that an increase in particle density is likely as particle mass decreases, and most reductions of micrometeoroid microphone and impact data (10,11) use values of density ranging from 0.5 to 3 grams/cm^3. These values of density for micrometeoroids (although never measured directly) indicate that the particles have a density of stoney materials. Thus, the Potter, Nebraska meteorite composition might be considered typical, and stoney type materials are therefore useful in micrometeoroid simulation studies.

To show the importance of $\bar{\rho}_\infty$ in predicting the reduction in reflectance of a polished metal for a given exposure energy, Eq. (1) is plotted in figure 5 for a 2024 aluminum sample with a value of $K = 0.297$/joule and values of $\bar{\rho}_\infty$ ranging from zero to 0.7. The value of K was determined from an expanded Eq. (1) that is not presented here, but is presented in Ref. 4 and includes the cratering energy density of the target. Knowing the cratering energy density of the target allows one to calculate K. However, K can be found empirically once the other values in Eq. (1) are found experimentally. Also plotted in figure 5 are measured values of $\bar{\rho}_f/\bar{\rho}_i$ for various exposures, where the ratio was found from the data points shown in figure 3 for the 2024 hard aluminum exposed to $\bar{6}$ μM SiC particles. For the curve with the value of $\bar{\rho}_\infty = 0.34$, the ultimate reflectance of 2024 aluminum after exposure to $\bar{6}$ μM SiC, the data points fit well on the predicted $\bar{\rho}_f/\bar{\rho}_i$ of Eq. (1). Figure 5 shows that knowing the correct value of $\bar{\rho}_\infty$ is important in getting the correct $\bar{\rho}_f/\bar{\rho}_i$ vs ε curve. However, for values of energy less than one joule (small exposures) changing the value of $\bar{\rho}_\infty$ by a factor of 2 changes the value of $\bar{\rho}_f/\bar{\rho}_i$ by about 10 percent. But, as the exposure energy gets larger, having the correct values of $\bar{\rho}_\infty$ becomes critically important in predicting the correct degradation rate.

Experiments using a polished metal or metal combination as a micrometeoroid flux detector as proposed in Ref. 12 are currently being flown on OSO III and SERT II. An added bonus from these studies is the indication that if no change in the thermal absorptance and emittance for a material to be flown in a micrometeoroid environment is desired the material can be exposed to simulated micrometeoroids on the ground until $\bar{\rho}_\infty$ is reached, and that this value can be expected not to change further.

CONCLUDING REMARKS

Different polished metals were quantitatively exposed to various types of hypervelocity stoney and metal projectiles until a value of $\bar{\rho}_\infty$ was reached for each projectile-target combination. Reflectance measurements of the exposed targets were made using a monochromator-integrating sphere and infrared spectrometer. It was found that for a given projectile the values of $\bar{\rho}_\infty$ were dependant of the target material, indicating that the ultimate reflectance does not become that of the impacting projectile. The polished metals exposed to the stoney type projectiles had almost the same value of $\bar{\rho}_\infty$ as the Potter, Nebraska meteorite, whereas the metallic type projectiles impacted against the same targets produced higher values of $\bar{\rho}_\infty$. This indicated that if the Potter, Nebraska meteorite is representative of the composition of real micrometeoroids in space, then stoney projectiles rather than metallic should be used in ground studies to simulate the effects of micrometeoroids on the optical properties of polished metals.

REFERENCES

1. Cosby, William A.; and Lyle, Robert G.: The Meteoroid Environment and Its Effects on Materials and Equipment. NASA SP-78, 1965.

2. Berg, Otto E.; and Gerloff, Ulrich: Orbital Elements of Micrometeorites Derived from Pioneer 8 Measurements. J. Geophys. Res., vol. 75, no. 34, Dec. 1, 1970, pp. 6932-6939.

3. Summers, James L.: Investigation of High-Speed Impact: Regions of Impact and Impact at Oblique Angles. NASA TN D-94, 1959.

4. Mirtich, Michael J.; and Mark, Herman: Feasibility of Accelerating Micron-Size Particles in Shock-Tube Flows for Hypervelocity Degradation of Reflective Surfaces. NASA TN D-3187, 1966.

5. Kornhauser, Maury: Prediction of Cratering by Meteoroid Impacts. Advances in Astronautical Sciences. Vol. 2. Norman V. Petersen and Horace Jacobs, eds., Plenum Press, 1958, pp. 33-1 - 33-13.

6. Eichelberger, R. J.: Hypervelocity Impact. Behavior of Materials Under Dynamic Loading. Norris J. Huffington, Jr., ed., ASME, 1965, pp. 155-187.

7. Bowman, R. L.; Mirtich, M. J.; and Weigand, A. J.: Changes in Optical Properties of Various Transmitting Materials Due to Simulated Micrometeoroid Exposure. Presented at the Optical Society of America Annual Meeting, Chicago, Ill., Oct. 21-24, 1969. TM X-52687.

8. Touloukian, Y. S., ed.: Thermophysical Properties of High Temperature Solid Material. Vol. 5. Macmillan Co., 1967, p. 139.

9. Verniani, F.: On the Density of Meteoroids. II-The Density of Faint Photographic Meteors. Nuovo Cimento, Ser. 10, vol. 33, no. 4, Aug. 16, 1964, pp. 1173-1184.

10. Alexander, W. M.; McCracken, C. W.; Secretan, L.; and Berg, O. E.: Review of Direct Measurements of Interplanetary Dust from Satellites and Probes. Goddard Space Flight Center Contributions to the Cospar Meeting May 1962. NASA TN D-1669, 1963, pp. 39-60.

11. Anon.: Meteoroid Environment Model-1969 (Near Earth to Lunar Surface). NASA SP-8013, 1969.

12. Mark, Herman; Sommers, Ralph D.; and Mirtich, Michael J.: Effect on Surface Thermal Properties of Calibrated Exposure to Micrometeoroid Environment. AIAA J., vol. 4, no. 10, Oct. 1966, pp. 1811-1817.

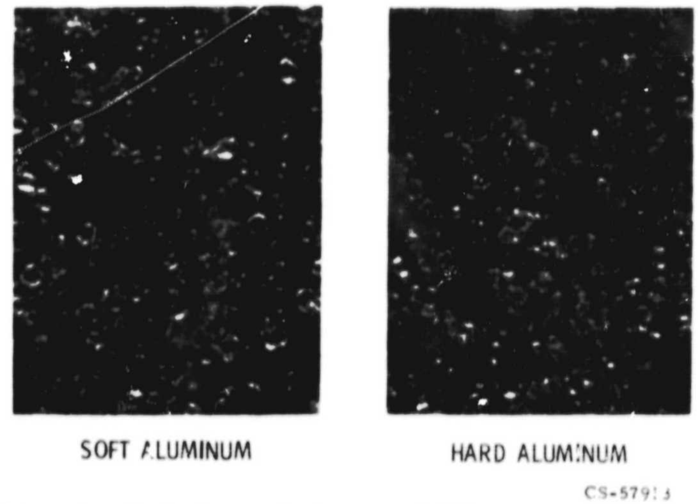

Figure 1. - Photomicrograph of surfaces (x315) exposed to (2-14) μSiC particles.

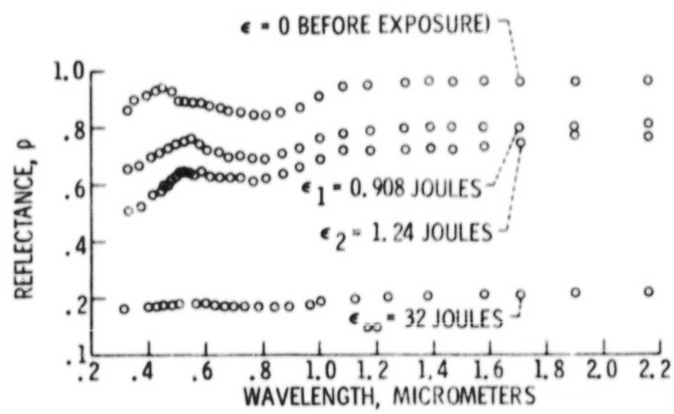

Figure 2. - Reflectance as a function of wavelength (0.33 to 2.16 μm) for a polished hard aluminum (7075) disk exposed to various exposure energies of $\bar{6}$μm SiC particles.

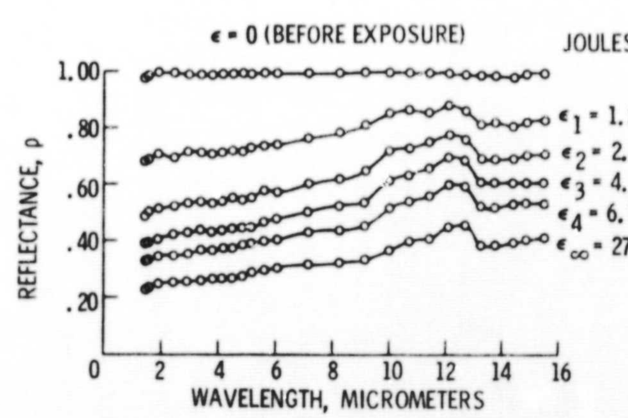

Figure 3. - Reflectance as a function of wavelength (1.5 to 15.5 μm) for a polished hard aluminum (2024) disk. Exposed to various exposure energies of $\bar{6}$μm SiC particles.

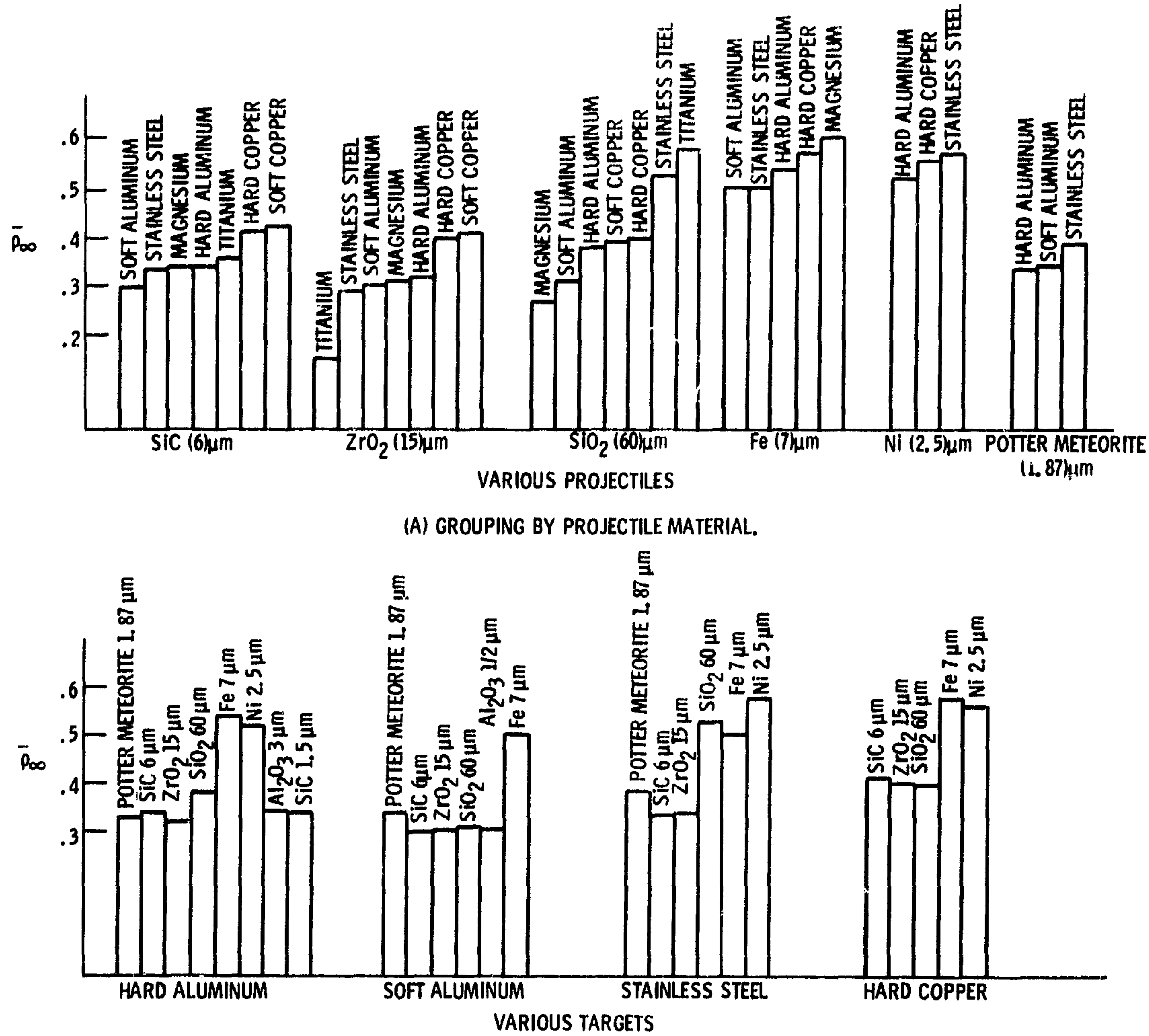

(A) GROUPING BY PROJECTILE MATERIAL.

(B) GROUPING BY TARGET MATERIAL.

Figure 4. - Normalized ultimate reflectance $\bar{\rho}_\infty$ for various projectile materials and target materials.

$$\frac{\rho_f}{\rho_i} = \left[1 - \left(1 - \frac{\rho_\infty}{\rho_i}\right)\left(1 - e^{-K\epsilon}\right)\right]$$

$K = 0.297$/JOULE

$\rho_i = 1.00$

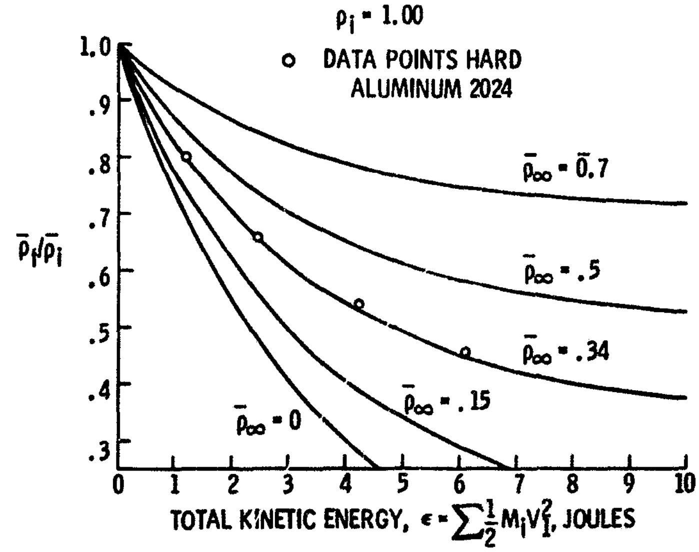

Figure 5. - Plot of reflectance ratio as a function of kinetic energy (eq. (1)) for a hard aluminum (2024) disk, with various values of $\bar{\rho}_\infty$.